Virus Research 201 (2015) 61–66

Contents lists available at ScienceDirect

Virus Research

journal homepage: www.elsevier.com/locate/virusres

MERS coronavirus envelope protein has a single transmembrane domain that forms pentameric ion channels

Wahyu Surya [a], Yan Li [a], Carmina Verdià-Bàguena [b], Vicente M. Aguilella [b], Jaume Torres [a,*]

[a] School of Biological Sciences, Nanyang Technological University, Singapore
[b] Department of Physics, Laboratory of Molecular Biophysics, Universitat Jaume I, 12071 Castellón, Spain

ARTICLE INFO

Article history:
Received 9 June 2014
Received in revised form 18 February 2015
Accepted 19 February 2015
Available online 27 February 2015

Keywords:
Middle East respiratory syndrome coronavirus (MERS)
Envelope protein
Ion channel
Purification
Oligomeric state

ABSTRACT

The Middle East respiratory syndrome coronavirus (MERS-CoV) is a newly identified pathogen able of human transmission that causes a mortality of almost 40%. As in the case of SARS-CoV, MERS virus lacking E protein represents a potential vaccine. In both cases, abolishment of channel activity may be a contributor to the attenuation observed in E-deleted viruses. Herein, we report that purified MERS-CoV E protein, like SARS-CoV E protein, is almost fully α-helical, has a single α-helical transmembrane domain, and forms pentameric ion channels in lipid bilayers. Based on these similarities, and the proposed involvement of channel activity as virulence factor in SARS-CoV E protein, MERS-CoV E protein may constitute a potential drug target.

1. Introduction

In September 2012 the first case of a novel coronavirus (CoV) infection was reported (Zaki et al., 2012) and the etiological agent was named Middle East respiratory syndrome coronavirus (MERS-CoV) (de Groot et al., 2013). As of 23 May 2014, 635 cases and 193 deaths have been confirmed (http://www.who.int/csr/don/2014_05_23_mers/en/). An investigation on 47 cases between September 2012 and June 2013 revealed that MERS patients display similar clinical features to severe acute respiratory syndrome (SARS) virus infection, but progress more rapidly towards respiratory failure (Assiri et al., 2013). In addition, a majority of MERS patients (estimated at 75%) has at least one co-morbid condition, in contrast to only 10–30% in SARS patients (Assiri et al., 2013; Drosten, 2013; Raj et al., 2014). Mortality rate in MERS-CoV-infected individuals is about 40%, compared to 10% during the SARS outbreak (http://www.who.int/csr/sarsarchive/2003_05_07a/en/). Human-to-human transmission has been reported, although it is still limited and inefficient (Raj et al., 2014). Although there are still no effective treatments, a mouse model suitable for studying MERS-CoV infection has been engineered (Zhao et al., 2014). The genomic sequence of MERS-CoV is closely related to bat CoVs HKU4 and HKU5, which belong to clade c of β-coronaviruses (Annan et al., 2013; Drexler et al., 2014). Like SARS-CoV, MERS-CoV is thought to have crossed over from bats to humans, although MERS-CoV used camels as an intermediate species (Haagmans et al., 2014).

The structural proteins in coronaviruses are N (nucleocapsid) and integral membrane proteins S (spike), M (membrane) and E (envelope). The S protein is involved in host recognition and entry into the cell. Recently, the crystal structure of the fusion core (Gao et al., 2013) and the receptor binding domain (Chen et al., 2013) of MERS S protein have been solved. The M protein is the most abundant protein in the lipid envelope of virions and defines their shape (Barcena et al., 2009; Neuman et al., 2011), although high resolution structural data is still not available. The E protein is scarcely present in the virion, but abundantly expressed in the infected cell, mainly distributed in intracellular membranes between ER and

Abbreviations: AQPZ, *E. coli* aquaporin Z; DDM, n-dodecyl β-D-maltoside; DHPC, 1,2-dihexanoyl-sn-glycero-3-phosphocholine; DMPC, 1,2-dimyristoyl-sn-glycero-3-phosphocholine; DPhPC, 1,2-diphytanoyl-sn-glycero-3-phosphocholine; DOPS, 1,2-dioleoyl-sn-glycero-3-phospho-L-serine; DPC, dodecyl phosphocholine; E, envelope; ER, endoplasmic reticulum; ERGIC, ER Golgi intermediate compartment; FTIR, Fourier-transform infrared spectroscopy; IBV, infectious bronchitis virus; LMPG, 1-myristoyl-2-hydroxy-sn-glycero-3-phosphoglycerol; M, membrane; MHV, murine hepatitis virus; MERS-CoV, Middle East respiratory syndrome coronavirus; N, nucleocapsid; POPC, 1-palmitoyl-2-oleoyl-sn-glycero-3-phosphocholine; SARS, severe acute respiratory syndrome; S, spike; SDS, sodium dodecyl sulphate; TM, transmembrane; TGEV, transmissible gastroenteritis virus.

* Corresponding author at: School of Biological Sciences, Nanyang Technological University, 60 Nanyang Drive, Singapore 637551, Singapore. Tel.: +65 6316 2857; fax: +65 6791 3856.
E-mail address: jtorres@ntu.edu.sg (J. Torres).

http://dx.doi.org/10.1016/j.virusres.2015.02.023
0168-1702/

Golgi compartments (Lim and Liu, 2001; Nal et al., 2005; Raamsman et al., 2000). In those sites, it participates in virus assembly, budding and intracellular trafficking. In the case of SARS-CoV, the E protein accumulates at the ERGIC (Nieto-Torres et al., 2011).

CoV E proteins are 76–109 amino acids long and predicted to have at least one α-helical transmembrane (TM) domain based on prediction algorithms (Surya et al., 2013). The extramembrane C-terminal domain has some hydrophobic character, and could represent in some cases a second TM domain, e.g., in infectious bronchitis virus (IBV) and in murine hepatitis virus (MHV) E proteins, although this has not been confirmed experimentally. SARS-CoV E protein has been shown unequivocally to have just one TM domain (Li et al., 2014), and is the only E protein for which structural data is available (Li et al., 2014; Pervushin et al., 2009). E proteins have been shown to form ion channels in synthetic membranes (Torres et al., 2007; Wilson et al., 2006), with reported conductance of 20–30 pS. However, characterization with properly purified full length and transmembrane peptides of SARS-CoV E protein has produced much higher (>10 times) conductances (Baguena et al., 2012; Verdia-Baguena et al., 2012, 2013a,b). In SARS-CoV, this channel activity has been linked to activation of caspase-1 and maturation of pro-inflammatory IL-1β during infection (Nieto-Torres et al., 2014), although a detailed mechanism to explain this functional link is still not available.

Removal of E protein is in general deleterious to coronaviruses, although the severity of the damage is strongly virus-dependent. For example, deletion of E gene in transmissible gastroenteritis virus (TGEV) results in blockage of virus trafficking in the cellular secretory pathway and prevention of virus maturation (Ortego et al., 2002). Mutations at the C-terminal region of MHV E protein results in impaired virion assembly and maturation (Fischer et al., 1998). SARS-CoV lacking the E gene is attenuated (DeDiego et al., 2007), and MERS-CoV lacking the E gene cannot propagate, despite showing similar viral RNA level to wild-type virus (Almazán et al., 2013). Based on the attenuating effect of E protein removal, a SARS-CoV lacking E gene is currently being studied as potential vaccine (Enjuanes et al., 2011; Fett et al., 2013; Netland et al., 2010), and a similar E-deletion approach has been suggested for controlling the MERS outbreak to obtain a virus that is replication-competent, but propagation-defective (Almazán et al., 2013).

The only coronavirus E protein structurally characterized in some detail is the one in SARS-CoV, as a transmembrane domain (Pervushin et al., 2009; Torres et al., 2006) and latter as a truncated form (residues 8–65), obtained using a 20 residue N-terminal tag that included a poly-His tail (Li et al., 2014). Herein, we report for the first time the expression, purification, and preliminary structural study on full-length 82 residue MERS-CoV E protein without any tag. This purified protein allowed its biophysical characterization to conclude that it has striking similarities to SARS-CoV E protein.

2. Materials and methods

2.1. Protein expression and purification

The DNA sequence encoding E protein from MERS-CoV-EMC12 (GenBank accession number JX869059) was fused N-terminally to a 6-His-MBP tag, followed by a TEV protease cleavage site, to form the construct 6-His-MBP-TEV-E. This was subcloned into pTB-MalE for expression. To investigate the effect of the four native cysteines (Fig. 1A), in addition to wild type MERS-CoV E, three additional Cys-to-Ala mutants were generated, at positions 23 and 30 (E_{AACC}), 40 and 43 (E_{CCAA}), and 23, 30, 40 and 43 (E_{AAAA}). Expression and purification of non labeled and ^{15}N-labeled E_{AAAA} was performed following the protocol described previously for MBP-tagged full-length SARS-COV E protein (Li et al., 2014), except that the elution buffer contained 1.6 mM n-dodecyl β-D-maltoside (DDM, Calbiochem).

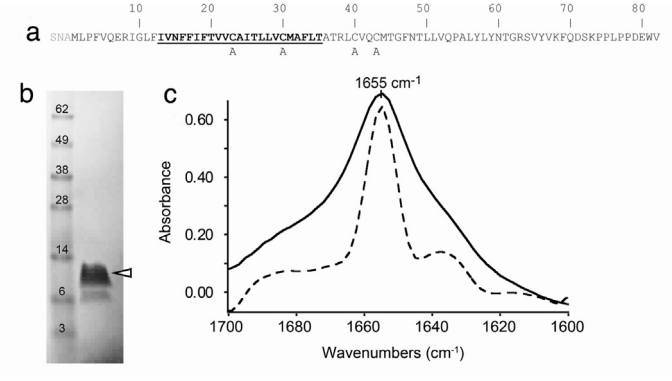

Fig. 1. Purification and secondary structure of MERS-CoV E protein. (A) Amino acid sequence of full-length E protein used in this study with predicted TM region in bold and underlined. The three N-terminal amino acids, SNA (gray), result from MBP tag removal by TEV protease cleavage. Positions of Cys residues, which were mutated into alanine, are indicated by 'A'; (B) SDS-NuPAGE of purified Cys-less mutant, E_{AAAA}. The protein band migrated approximately at its calculated molecular weight of 9.6 kDa; (C) infrared amide I region of MERS-CoV E in hydrated POPC lipid bilayers (solid line) and its corresponding Fourier self-deconvolved spectrum (dashed line).

2.2. Gel electrophoresis

For SDS-NuPAGE, samples were run in 4–12% NuPAGE® Bis–Tris gels (Invitrogen) with NuPAGE® MES SDS running buffer and stained with SimplyBlue™ SafeStain (Invitrogen) according to the manufacturer's protocol. Blue-native PAGE (BN-PAGE) was performed as described previously (Gan et al., 2011). Lyophilized peptide was solubilized to 0.1 mM in a sample buffer containing 50 mM DHPC (Avanti Polar Lipids), 5, 25 and 50 mM DPC (Avanti Polar Lipids), or 21 mM LMPG (Anatrace). *Escherichia coli* aquaporin Z (AqpZ) in 20 mM SDS was included as additional molecular weight marker.

2.3. Fourier-transform infrared spectroscopy

Sample preparation, ATR data collection and H/D exchange were performed as described previously (Torres et al., 2006) on a Nicolet Nexus spectrometer (Madison, USA). Briefly, the peptide was incorporated in multilamellar liposomes by dissolving a dry mixture of peptide and POPC (Avanti Polar Lipids) or DMPC (Avanti Polar Lipids) at a 1:50 molar ratio. Fourier self-deconvolution was performed on the amide I region using FWHH of 20 cm^{-1} and a narrowing factor k of 1.5 (Kauppinen et al., 1981).

2.4. Analytical ultracentrifugation

Sedimentation equilibrium data were collected at 20 °C in a Beckman XL-I analytical ultracentrifuge monitoring the absorbance at 280 nm. Lyophilized peptide was dissolved to OD_{280} of 0.3, 0.5, and 0.8 (12 mm pathlength) in 50 mM Tris buffer (pH 7.3), 100 mM NaCl, 5 mM C14-betaine and 32.3% D_2O. The samples were centrifuged in six-channel charcoal-filled Epon centerpieces with quartz windows. Radial distribution profiles were acquired at 18,500, 22,700, and 27,800 rpm after reaching equilibrium. The latter was tested by HeteroAnalysis. Data were processed and fitted to several monomer-N-mer models in SEDFIT and SEDPHAT (Schuck, 2003).

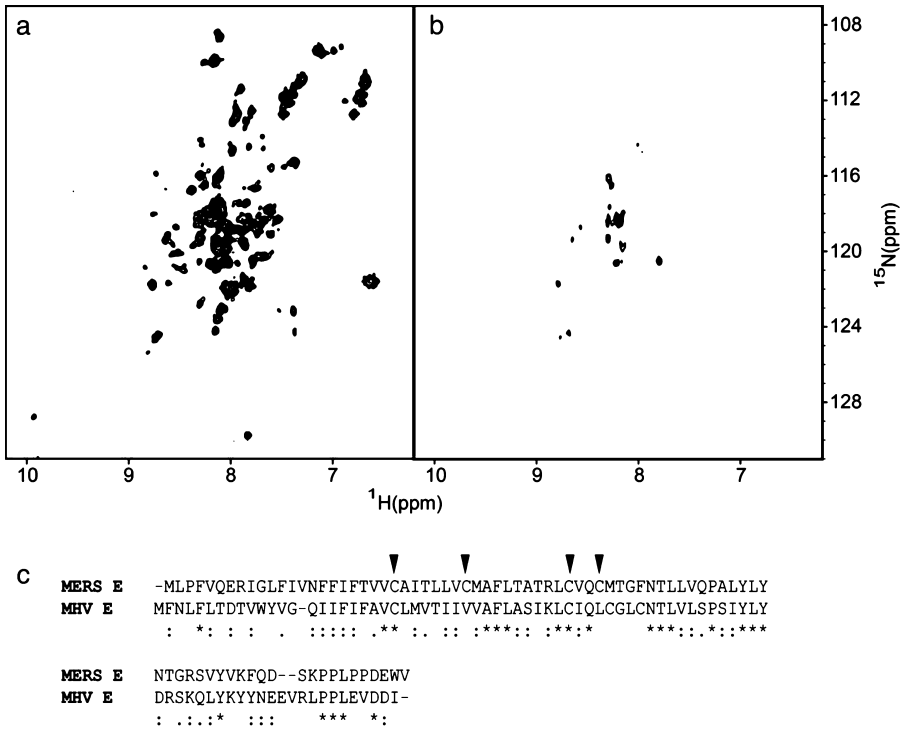

Fig. 2. HSQC spectrum of ^{15}N-labeled MERS-CoV E protein. (A) [^{1}H–^{15}N]-HSQC spectrum of 0.2 mM MERS-CoV E in 200 mM SDS micelles dissolved in H_2O; (B) same as (A), after exposure to 99% D_2O; (C) alignment of E proteins from MERS-CoV and MHV. The position of the four Cys residues in MERS-CoV E is indicated.

2.5. Conductance measurements

The experiments reported here have been carried out in single ion channels reconstituted on planar membranes. Planar bilayer membranes were formed from two monolayers prepared from a lipid mixture containing 1,2-dioleoyl-*sn*-glycero-3-phpsphocoline (DOPC), 1,2-di-(9Z-octadecenoyl)-*sn*-glycero-3-phospho-L-serine (DOPS) and 1,2-dioleoyl-*sn*-glycero-3-phosphoethanolamine (DOPE) at a 3:1:1 (DOPC:DOPS:DOPE) in pentane on 70–90 μm diameter orifices in the 15 μm-thick Teflon partition that separated two identical chambers (Bezrukov and Vodyanoy, 1993; Montal and Mueller, 1972). The orifices were pretreated with a 1% solution of hexadecane in pentane. Aqueous solutions of KCl and NaCl were buffered with 5 mM HEPES at pH 6. All measurements were performed at room temperature. Single channel insertion was achieved by adding 2–3 μL of a 150 μg/mL solution of protein in the buffer that contains acetonitrile:isopropanol (40:60) at the cis side of the chamber.

An electric potential was applied using Ag/AgCl electrodes in 2 M KCl, 1.5% agarose bridges assembled within standard 250 ml pipette tips. The potential was defined as positive when it was higher on the side of the protein addition (the *cis* side of the membrane chamber), whereas the *trans* side was set to ground. An Axopatch 200B amplifier (Molecular Devices, Sunnyvale, CA) in the voltage-clamp mode was used to measure the current and applied potential. The chamber and the head stage were isolated from external noise sources with a double metal screen (Amuneal Manufacturing Corp., Philadelphia, PA). The single-channel conductance was obtained from the current measurement at applied potential of +100 mV in symmetrical salt solutions.

2.6. NMR spectroscopy

NMR experiments were performed at 318 K using an Avance-II 600 NMR spectrometer with a cryogenic probe. Sodium 2,2-dimethyl-2-silapentane-5-sulfonate (DSS) was used as the internal reference for ^{1}H nuclei. The chemical shifts of ^{15}N nuclei were calculated from the ^{1}H chemical shifts. The NMR data were processed using TopSpin 3.1 (www.bruker-biospin.com) and analyzed using CARA (www.nmr.ch). To identify membrane-embedded residues, the NMR sample was lyophilized overnight and reconstituted in 99% D_2O. Immediately after reconstitution, a 2D [^{1}H–^{15}N]-HSQC spectrum was collected.

3. Results and discussion

3.1. Expression and purification of MERS-CoV E protein

Full length MERS-CoV E protein was successfully expressed as a fusion protein with maltose binding protein (MBP) attached to the N-terminus of E. MBP was subsequently removed by TEV protease, leaving behind additional 3 residues, SNA, at the N terminus of MERS-CoV E protein (Fig. 1A). Four mutants were tested (see Section 2), but only a Cys-null mutant (E_{AAAA}) could be obtained with sufficient purity, which was further characterized. This mutant is referred to hereafter as 'MERS-CoV E protein'. The purity of this mutant was at least 90% after reverse-phase HPLC purification, as shown by gel SDS electrophoresis (Fig. 1B). When reconstituted in POPC lipid bilayers, the polypeptide was predominantly α-helical, as indicated by an infrared amide I band centered at 1655 cm^{-1} (Fig. 1C). These spectral features are also common to SARS-CoV E protein (Li et al., 2014), which suggests a similar overall secondary structure.

3.2. MERS-CoV E has a single TM domain

Screening of MERS-CoV E protein in micellar and bicellar environments identified SDS as the best detergent to achieve good peak dispersion in the two dimensions of an [^{1}H–^{15}N]-HSQC spectrum (Fig. 2A), implying foldedness and lack of aggregation. We note that although this SDS environment will not allow the formation of oligomers (Fig. 1B), it is nevertheless likely to produce near-native

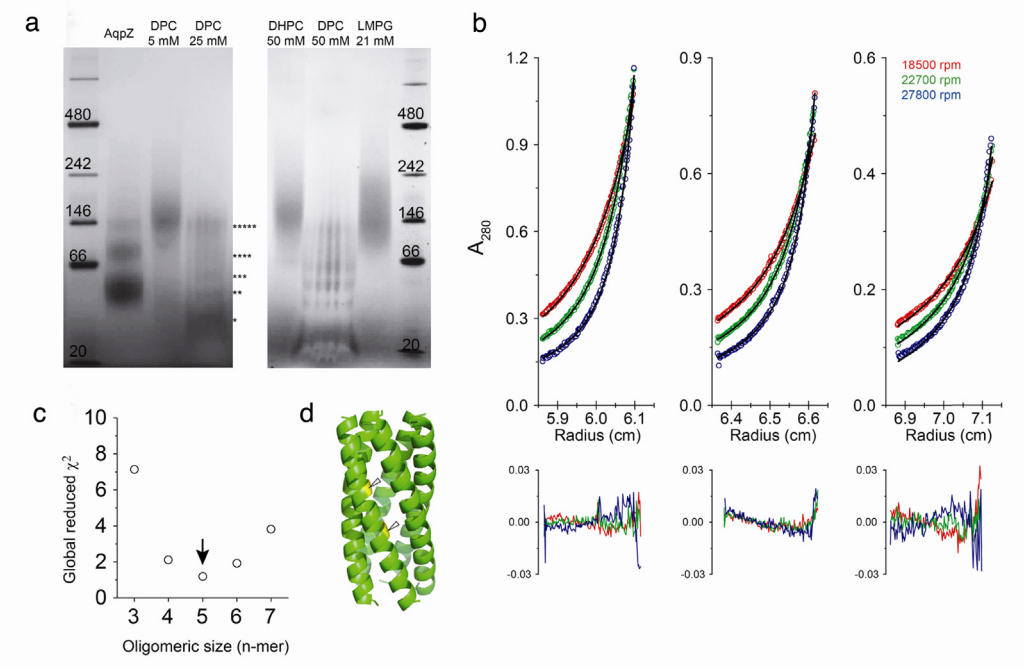

Fig. 3. Oligomeric state of MERS-CoV E protein. (A) Blue-native PAGE of 0.1 mM MERS-CoV E protein at the indicated concentrations of DPC, DHPC, and LMPG detergents. Oligomeric sizes are indicated by asterisks; (B) radial distribution profiles of the protein solubilized in C14-betaine micelles (open dots) and fitting to a monomer–pentamer self-association model (solid line) at the angular speeds shown. Residuals of the fitting are shown in the lower panel; (C) Chi-squared values corresponding to fitting to different monomer: n-mer models, from trimers to heptamers. The most optimal fit (monomer–pentamer) is indicated by an arrow; (D) homo-pentameric model of the TM domain of SARS-CoV E protein. The *equivalent* positions of the two Cys residues in MERS-CoV E protein, mutated in the present work, are highlighted (yellow, arrows) and shown at an interfacial orientation. (For interpretation of the references to color in this figure legend, the reader is referred to the web version of this article.)

secondary structure. This assumption is based on results obtained previously for SARS-CoV E protein (Li et al., 2014), where titration of the polypeptide SDS with increasing DPC, up to a 1:4 SDS/DPC molar ratio, did not lead to changes in secondary structure, as monitored by $^{13}C_{\alpha}$ chemical shifts.

To determine if MERS-CoV E protein has one or two TM domains, the membrane-embedded residues were quantified using [^{1}H–^{15}N]-HSQC spectra in an H^{N}-D_2O exchange experiment. In 99% D_2O, ~20 residues were found to be protected from exchange (Fig. 2B), which suggests a single α-helical TM domain.

Early studies of N- or C-terminally tagged MHV E (Maeda et al., 2001) and SARS-CoV E (Yuan et al., 2006) proposed that both N and C-terminal ends were facing the cytoplasm, with the implication of two TM domains. However, purified full length SARS-CoV E protein has only one TM domain, as shown in a H^{N}-D_2O exchange experiment (Li et al., 2014). In addition, the topology of untagged SARS-CoV E protein, both in SARS-infected cells and transfected cells shows that only one TM domain is possible, with C-terminal and N-terminal ends located cytoplasmically and lumenally, respectively (Nieto-Torres et al., 2011). The high sequence similarity between MERS-CoV and MHV E proteins (Fig. 2C) further suggests that the latter also has one α-helical TM domain.

3.3. MERS-CoV E protein forms pentamers

We have shown previously that SARS-CoV E protein forms homo-pentamers (Li et al., 2014; Parthasarathy et al., 2012). To test if MERS-CoV E protein also forms pentamers, Blue-native PAGE electrophoresis and sedimentation experiments were performed. When MERS-CoV E protein was solubilized in 5 mM DPC micelles (1:50 protein-to-detergent molar ratio) it migrated as a single band in a BN-PAGE gel (Fig. 3A). In common with other membrane proteins (Gan et al., 2011), the molecular weight of this band may not correspond to the molecular weight markers used, or to the AQPZ ladder (~25 kDa for the monomer) possibly because of residual detergent bound to the protein. However, after dilution with 25 mM DPC, MERS-CoV E protein dissociated into lower molecular weight oligomers, from monomers to pentamers (Fig. 3A). This ladder conveniently provides an internal reference that serves as a oligomeric size marker. Therefore, by comparison with that ladder, we confidently assign the single band observed in 5 mM DPC to pentameric oligomers. The same oligomeric size was observed when using 50 mM DHPC and 20 mM LMPG (Fig. 3A, right panel), which are potentially good environments for structural characterization.

The oligomeric state of E protein was further confirmed by using analytical ultracentrifugation. MERS-CoV E protein was solubilized in 5 mM C14-betaine micelles at the concentrations described in Section 2. Sedimentation equilibrium data could be best fitted to a monomer–pentamer self-association reversible model (Fig. 3B and C) with apparent association constant, K_a, of 6.3×10^{17} M^{-4} ($\text{Log}\,K_a = 17.8$). This is almost identical to the value ($\text{Log}\,K_a = 17.5$) obtained in C14-betaine for the full length wild type SARS-CoV E protein in presence of reductant TCEP (Parthasarathy et al., 2012). These values are one order of magnitude higher than those obtained for truncated Cys-less SARS-CoV E protein (residues 8–65) (Li et al., 2014) although the latter contained a relatively long (20 residues) N-terminal tag, which may have affected the stability of the pentamer.

A total of four cysteines are present in the wild-type MERS-CoV E protein sequence, two in the predicted TM domain and two in the predicted C-terminal juxtamembrane region (Fig. 1). The above results suggest that the introduced Cys-to-Ala mutations in the TM domain do not affect oligomer stability. Assuming that the mutual orientation between the TM helices is the same in all CoV E proteins, and therefore to that of SARS-CoV E protein (Pervushin et al., 2009; Torres et al., 2005, 2006), the orientation of the two TM cysteines in MERS-CoV E can be assumed to be near the helix–helix interface (Fig. 3D). The TM helix–helix orientation of coronavirus E

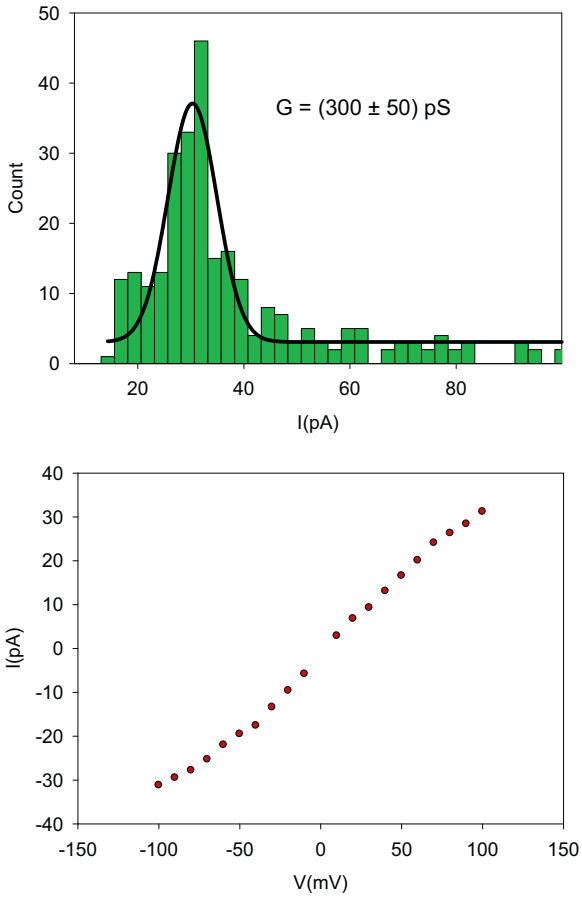

Fig. 4. Conductance measurements of MERS-CoV E protein in lipid bilayers. (A) Histogram corresponding to the current jump amplitudes at +100 mV for MERS E protein, fitted to a Gaussian model. Experiments were carried out in 500 mM KCl solutions at pH 6 in membranes containing 3:1:1 DOPC:DOPE:DOPS. The histogram contains 300 events; (B) MERS E protein current–voltage relationship. This experiment is for a single channel, i.e., one experiment which showed almost no deviation.

proteins has been recently validated by in vivo data, where revertant mutants of SARS-CoV were obtained in mice after introducing a channel-inactivating mutation V25F in its E protein. This mutation was located at an interhelical position in our pentameric model, whereas the mutations that recovered channel activity were at positions 37, 30, 26, 27 and 19, all located at the helix–helix interface and facing V25F (Nieto-Torres et al., 2014). The two cysteines at the TM domain of MERS-CoV E are equivalent to positions 30 and 23 in the SARS-CoV E protein. Despite this putative inter-helical orientation, these Cys-to-Ala mutations did not seem to affect oligomer size or stability.

3.4. MERS-CoV E protein displays ion channel activity in lipid bilayers

Conductance histograms of recorded traces at +100 mV are shown in Fig. 4A. We can observe that MERS E protein forms an ion channel with conductance of 0.3 ± 0.01 nS in 1 M KCl. The channel displays ohmic behavior (Fig. 4B). These value is comparable to those obtained for purified truncated SARS-CoV E protein in the same conditions (Li et al., 2014), where conductance was 0.39 ± 0.02 nS. Synthetic full length SARS-CoV E protein and synthetic transmembrane domain of SARS-CoV E (E_{TM}, residues 7–38) produced single channel conductances of 0.19 ± 0.06 pS and 0.18 ± 0.12 nS in 1 M NaCl (Verdia-Baguena et al., 2012), although these lower values may have been due to modifications introduced during synthesis or to impurities.

In conclusion, we show that MERS-CoV E protein can be efficiently purified and, like SARS-CoV E protein, forms homopentamers where each monomer has a single TM domain. The substitution Cys-to-Ala in the two native TM Cys residues seems well tolerated and does not affect the pentamer stability or channel activity significantly, even though these residues should be located at or near the helix–helix interface. The good behavior of this construct in detergent enables structural characterization that is in progress, as well as drug binding biophysical assays.

Acknowledgements

We thank Dr. Luis Enjuanes for the gift of the plasmid carrying MERS-CoV E cDNA. This work has been funded by the Singapore National Research Foundation under CRP Award No. NRF-CRP4-2008-02 and Tier 1 grant RG 51/13.

References

Almazán, F., DeDiego, M.L., Sola, I., Zuñiga, S., Nieto-Torres, J.L., Marquez-Jurado, S., Andrés, G., Enjuanes, L., 2013. Engineering a replication-competent, propagation-defective Middle East respiratory syndrome coronavirus as a vaccine candidate. MBio 4 (5).

Annan, A., Baldwin, H.J., Corman, V.M., Klose, S.M., Owusu, M., Nkrumah, E.E., Badu, E.K., Anti, P., Agbenyega, O., Meyer, B., Oppong, S., Sarkodie, Y.A., Kalko, E.K.V., Lina, P.H.C., Godlevska, E.V., Reusken, C., Seebens, A., Gloza-Rausch, F., Vallo, P., Tschapka, M., Drosten, C., Drexler, J.F., 2013. Human betacoronavirus 2c EMC/2012-related viruses in bats, Ghana and Europe. Emerg. Infect. Dis. 19 (3), 456–459.

Assiri, A., Al-Tawfiq, J.A., Al-Rabeeah, A.A., Al-Rabiah, F.A., Al-Hajjar, S., Al-Barrak, A., Flemban, H., Al-Nassir, W.N., Balkhy, H.H., Al-Hakeem, R.F., Makhdoom, H.Q., Zumla, A.I., Memish, Z.A., 2013. Epidemiological, demographic, and clinical characteristics of 47 cases of Middle East respiratory syndrome coronavirus disease from Saudi Arabia: a descriptive study. Lancet Infect. Dis. 13 (9), 752–761.

Baguena, C.V., Nieto-Torres, J.L., Alcaraz, A., DeDiego, M.L., Enjuanes, L., Aguilella, V.M., 2012. On channel activity of synthetic peptides derived from severe and acute respiratory syndrome coronavirus (SARS-CoV) E protein. Biophys. J. 102 (3), 656a–657a.

Barcena, M., Oostergetel, G.T., Bartelink, W., Faas, F.G., Verkleij, A., Rottier, P.J., Koster, A.J., Bosch, B.J., 2009. Cryo-electron tomography of mouse hepatitis virus: insights into the structure of the coronavirion. Proc. Natl. Acad. Sci. U. S. A. 106 (2), 582–587.

Bezrukov, S.M., Vodyanoy, I., 1993. Probing alamethicin channels with water-soluble polymers – effect on conductance of channel states. Biophys. J. 64 (1), 16–25.

Chen, Y., Rajashankar, K.R., Yang, Y., Agnihothram, S.S., Liu, C., Lin, Y.L., Baric, R.S., Li, F., 2013. Crystal structure of the receptor-binding domain from newly emerged Middle East respiratory syndrome coronavirus. J. Virol. 87 (19), 10777–10783.

de Groot, R.J., Baker, S.C., Baric, R.S., Brown, C.S., Drosten, C., Enjuanes, L., Fouchier, R.A.M., Galiano, M., Gorbalenya, A.E., Memish, Z.A., Perlman, S., Poon, L.L.M., Snijder, E.J., Stephens, G.M., Woo, P.C.Y., Zaki, A.M., Zambon, M., Ziebuhr, J., 2013. Middle East respiratory syndrome coronavirus (MERS-CoV): announcement of the Coronavirus Study Group. J. Virol. 87 (14), 7790–7792.

DeDiego, M.L., Alvarez, E., Almazan, F., Rejas, M.T., Lamirande, E., Roberts, A., Shieh, W.J., Zaki, S.R., Subbarao, K., Enjuanes, L., 2007. A severe acute respiratory syndrome coronavirus that lacks the E gene is attenuated in vitro and in vivo. J. Virol. 81 (4), 1701–1713.

Drexler, J.F., Corman, V.M., Drosten, C., 2014. Ecology, evolution and classification of bat coronaviruses in the aftermath of SARS. Antiviral Res. 101, 45–56.

Drosten, C., 2013. Is MERS another SARS? Lancet Infect. Dis. 13 (9), 727–728.

Enjuanes, L., Nieto-Torres, J.L., Jimenez-Guardeno, J.M., DeDiego, M.L., 2011. Recombinant live vaccines to protect against the severe acute respiratory syndrome coronavirus. In: al, P.R.D.e. (Ed.), Replicating Vaccines, Birkhauser Advances in Infectious Diseases. Springer, Basel, pp. 73–97.

Fett, C., DeDiego, M.L., Regla-Nava, J.A., Enjuanes, L., Perlman, S., 2013. Complete protection against severe acute respiratory syndrome coronavirus-mediated lethal respiratory disease in aged mice by immunization with a mouse-adapted virus lacking E protein. J. Virol. 87 (12), 6551–6559.

Fischer, F., Stegen, C.F., Masters, P.S., Samsonoff, W.A., 1998. Analysis of constructed E gene mutants of mouse hepatitis virus confirms a pivotal role for E protein in coronavirus assembly. J. Virol. 72 (10), 7885–7894.

Gan, S.W., Vararattanavech, A., Nordin, N., Eshaghi, S., Torres, J., 2011. A cost-effective method for simultaneous homo-oligomeric size determination and monodispersity conditions for membrane proteins. Anal. Biochem. 416 (1), 100–106.

Gao, J., Lu, G., Qi, J., Li, Y., Wu, Y., Deng, Y., Geng, H., Li, H., Wang, Q., Xiao, H., Tan, W., Yan, J., Gao, G.F., 2013. Structure of the fusion core and inhibition of fusion by a heptad repeat peptide derived from the S protein of middle east respiratory syndrome coronavirus. J. Virol. 87 (24), 13134–13140.

Haagmans, B.L., Al Dhahiry, S.H.S., Reusken, C.B.E.M., Raj, V.S., Galiano, M., Myers, R., Godeke, G.-J., Jonges, M., Farag, E., Diab, A., Ghobashy, H., Alhajri, F., Al-Thani, M., Al-Marri, S.A., Al Romaihi, H.E., Al Khal, A., Bermingham, A., Osterhaus, A.D.M.E., AlHajri, M.M., Koopmans, M.P.G., 2014. Middle East respiratory syndrome coronavirus in dromedary camels: an outbreak investigation. Lancet Infect. Dis. 14 (2), 140–145.

Kauppinen, J.K., Moffatt, D.J., Cameron, D.G., Mantsch, H.H., 1981. Noise in Fourier self-deconvolution. Appl. Opt. 20 (10), 1866–1879.

Li, Y., Surya, W., Claudine, S., Torres, J., 2014. Structure of a conserved Golgi complex-targeting signal in coronavirus envelope proteins. J. Biol. Chem. 289 (18), 12535–12549.

Lim, K.P., Liu, D.X., 2001. The missing link in coronavirus assembly. Retention of the avian coronavirus infectious bronchitis virus envelope protein in the pre-Golgi compartments and physical interaction between the envelope and membrane proteins. J. Biol. Chem. 276 (20), 17515–17523.

Maeda, J., Repass, J.F., Maeda, A., Makino, S., 2001. Membrane topology of coronavirus E protein. Virology 281 (2), 163–169.

Montal, M., Mueller, P., 1972. Formation of bimolecular membranes from lipid monolayers and a study of their electrical properties. Proc. Natl. Acad. Sci. U. S. A. 69 (12), 3561–3566.

Nal, B., Chan, C., Kien, F., Siu, L., Tse, J., Chu, K., Kam, J., Staropoli, I., Crescenzo-Chaigne, B., Escriou, N., van der Wef, S., Yuen, K.-Y., Altmeyer, R., 2005. Differential maturation and subcellular localization of severe acute respiratory syndrome coronavirus surface proteins S, M and E. J. Gen. Virol. 86 (5), 1423–1434.

Netland, J., DeDiego, M.L., Zhao, J.C., Fett, C., Alvarez, E., Nieto-Torres, J.L., Enjuanes, L., Perlman, S., 2010. Immunization with an attenuated severe acute respiratory syndrome coronavirus deleted in E protein protects against lethal respiratory disease. Virology 399 (1), 120–128.

Neuman, B.W., Kiss, G., Kunding, A.H., Bhella, D., Baksh, M.F., Connelly, S., Droese, B., Klaus, J.P., Makino, S., Sawicki, S.G., Siddell, S.G., Stamou, D.G., Wilson, I.A., Kuhn, P., Buchmeier, M.J., 2011. A structural analysis of M protein in coronavirus assembly and morphology. J. Struct. Biol. 174 (1), 11–22.

Nieto-Torres, J.L., DeDiego, M.L., Alvarez, E., Jimenez-Guardeno, J.M., Regla-Nava, J.A., Llorente, M., Kremer, L., Shuo, S., Enjuanes, L., 2011. Subcellular location and topology of severe acute respiratory syndrome coronavirus envelope protein. Virology 415 (2), 69–82.

Nieto-Torres, J.L., Dediego, M.L., Verdia-Baguena, C., Jimenez-Guardeno, J.M., Regla-Nava, J.A., Fernandez-Delgado, R., Castano-Rodriguez, C., Alcaraz, A., Torres, J., Aguilella, V.M., Enjuanes, L., 2014. Severe acute respiratory syndrome coronavirus envelope protein ion channel activity promotes virus fitness and pathogenesis. PLoS Pathog. 10 (5), e1004077.

Ortego, J., Escors, D., Laude, H., Enjuanes, L., 2002. Generation of a replication-competent, propagation-deficient virus vector based on the transmissible gastroenteritis coronavirus genome. J. Virol. 76 (22), 11518–11529.

Parthasarathy, K., Lu, H., Surya, W., Vararattanavech, A., Pervushin, K., Torres, J., 2012. Expression and purification of coronavirus envelope proteins using a modified β-barrel construct. Protein Expr. Purif. 85 (1), 133–141.

Pervushin, K., Tan, E., Parthasarathy, K., Lin, X., Jiang, F.L., Yu, D., Vararattanavech, A., Soong, T.W., Liu, D.X., Torres, J., 2009. Structure and inhibition of the SARS coronavirus envelope protein ion channel. PLoS Pathog. 5 (7), e1000511.

Raamsman, M.J., Locker, J.K., de Hooge, A., de Vries, A.A., Griffiths, G., Vennema, H., Rottier, P.J., 2000. Characterization of the coronavirus mouse hepatitis virus strain A59 small membrane protein E. J. Virol. 74 (5), 2333–2342.

Raj, V.S., Osterhaus, A.D.M.E., Fouchier, R.A.M., Haagmans, B.L., 2014. MERS: emergence of a novel human coronavirus. Curr. Opin. Virol. 5 (0), 58–62.

Schuck, P., 2003. On the analysis of protein self-association by sedimentation velocity analytical ultracentrifugation. Anal. Biochem. 320 (1), 104–124.

Surya, W., Samsó, M., Torres, J., 2013. Structural and functional aspects of viroporins in human respiratory viruses: respiratory syncytial virus and coronaviruses. In: Vats, M. (Ed.), Respiratory Disease and Infection – A New Insight. InTech, pp. 47–76.

Torres, J., Maheswari, U., Parthasarathy, K., Ng, L., Ding, X.L., Gong, X., 2007. Conductance and amantadine binding of a pore formed by a lysine-flanked transmembrane domain of SARS coronavirus envelope protein. Protein Sci. 16 (9), 2065–2071.

Torres, J., Parthasarathy, K., Lin, X., Saravanan, R., Kukol, A., Liu, D.X., 2006. Model of a putative pore: the pentameric α-helical bundle of SARS coronavirus E protein in lipid bilayers. Biophys. J. 91, 938–947.

Torres, J., Wang, J., Parthasarathy, K., Liu, D.X., 2005. The transmembrane oligomers of coronavirus protein E. Biophys. J. 88 (2), 1283–1290.

Verdia-Baguena, C., Nieto-Torres, J.L., Alcaraz, A., DeDiego, M.L., Enjuanes, L., Aguilella, V.M., 2013a. Analysis of SARS-CoV E protein ion channel activity by tuning the protein and lipid charge. Biochim. Biophys. Acta-Biomembr. 1828 (9), 2026–2031.

Verdia-Baguena, C., Nieto-Torres, J.L., Alcaraz, A., DeDiego, M.L., Enjuanes, L., Aguilella, V.M., 2013b. Channels formed by SARS coronavirus envelope protein: lipid regulation of conductance and selectivity. Biophys. J. 104 (2), 632a-632a.

Verdia-Baguena, C., Nieto-Torres, J.L., Alcaraz, A., DeDiego, M.L., Torres, J., Aguilella, V.M., Enjuanes, L., 2012. Coronavirus E protein forms ion channels with functionally and structurally-involved membrane lipids. Virology 432 (2), 485–494.

Wilson, L., Gage, P., Ewart, G., 2006. Hexamethylene amiloride blocks E protein ion channels and inhibits coronavirus replication. Virology 353 (2), 294–306.

Yuan, Q., Liao, Y., Torres, J., Tam, J.P., Liu, D.X., 2006. Biochemical evidence for the presence of mixed membrane topologies of the severe acute respiratory syndrome coronavirus envelope protein expressed in mammalian cells. FEBS Lett. 580, 3192–3200.

Zaki, A.M., Van Boheemen, S., Bestebroer, T.M., Osterhaus, A.D.M.E., Fouchier, R.A.M., 2012. Isolation of a novel coronavirus from a man with pneumonia in Saudi Arabia. N. Engl. J. Med. 367 (19), 1814–1820.

Zhao, J.C., Li, K., Wohlford-Lenane, C., Agnihothram, S.S., Fett, C., Zhao, J.X., Gale, M.J., Baric, R.S., Enjuanes, L., Gallagher, T., McCray, P.B., Perlman, S., 2014. Rapid generation of a mouse model for Middle East respiratory syndrome. Proc. Natl. Acad. Sci. U. S. A. 111 (13), 4970–4975.